Calcified Particles From Human Aortae Modulate Human Aortic Valvular Cells

Van Engeland

Short title: Calcified particles modulate aortic valvular cells

Nicole van Engeland[1,2], MSc, Sergio Bertazzo[3], PhD, Padmini Sarathchandra[1], PhD, Ann McCormack[1], BSc, Carlijn Bouten[2], PhD, Magdi H Yacoub[1], FRCS, Adrian H Chester[1], PhD and Najma Latif[1], PhD

Imperial College London[1], Heart Science Centre, Harefield Hospital, Harefield, Middlesex UB9 6JH, UK, Technical University of Eindhoven[2], Department of Biomedical Engineering, 5600 MB Eindhoven, the Netherlands; University College London[3], Department of Medical Physics & Biomedical Engineering, Malet Place Engineering Building, London WC1E 6BT, UK

Address for correspondence:

N Latif, Imperial College, Heart Science Centre, Harefield Hospital, Harefield, Middx. UB9 6JH

Tel no: 0044 1895 453846

E-mail: n.latif@imperial.ac.uk

Total word count: 7097

Abstract

Background: Recently, using nano-analytical electron microscopy, we showed that human valve cusps, coronary arteries and aortae, with and without calcific disease, harbour spherical calcium phosphate micro-particles of the identical composition and crystallinity. Importantly these calcified particles were present prior to any clinical sign of calcification and as yet, their role remains unknown. Objective: To examine the direct effects of isolated calcified particles on human valvular cells.

Methods: Calcified particles were isolated from healthy and diseased aortae using collagenase and hydrazine and characterized by scanning electron microscopy and energy dispersive x-ray spectroscopy. The calcified particles were quantitated by turbidity and applied to a monoculture of valvular endothelial cells (VECs) and interstitial cells (VICs) by adding them directly into the media. Cell differentiation, viability and proliferation was analysed. Results: Particles were heterogeneous differing in size and shape and were crystallized as calcium phosphate. There was a significant difference in the amount of calcified particles isolated from diseased donors compared to healthy donors ($p<0.05$), but there were no differences between the composition of the particles from healthy and diseased donors. VECs treated with calcified particles showed a significant decrease in CD31, VE-cadherin and an increase in von Willebrand Factor (vWF) expression, $p<0.05$, when treated with calcified particles for three weeks. There was a significant increase in α-SMA and osteopontin ($p<0.05$), with increased expression of alizarin red and von Kossa in VICs when treated with the particles for three weeks. VEC and VIC viability was significantly decreased by the calcified particles ($p<0.05$) with a significantly increased number of TUNEL positive VECs ($p<0.05$) indicating apoptosis. Proliferative capacity of VECs and VICs after 14 days incubation with calcified particles was unchanged.

Conclusion: Isolated calcified particles from human aortae are not innocent bystanders but induce a phenotypical and pathological change of VECs and VICs characteristic of activated

and osteoblast-like cells. Therapy tailored to reduce these calcified particles should be investigated.

Key words: calcified particles, valve endothelial cells, valve interstitial cells, osteogenesis, endothelial-to-mesenchymal transformation.

Abbreviations:

VEC: valve endothelial cell

VIC: valve interstitial cell

CAVD: calcific aortic valve disease

SEM: scanning electron microscopy

vWF: vonWillebrand Factor

TGFβ1: transforming growth factor 1

Introduction

Calcification is a widespread phenomenon involved in several cardiovascular diseases such as calcific aortic valve disease (CAVD) and atherosclerosis [1]. CAVD is a slowly progressive disorder of dysregulated calcium deposition, very common in the elderly. It is found in 26% of the population over the age of 65 [2, 3], 35% between 75 and 84 years of age, and up to 50% of those over 85 [4, 5]. CAVD ranges from mild valve thickening without obstruction of blood flow, known as aortic sclerosis, to severe calcification with impaired leaflet motion, termed aortic stenosis.

The pathological pathways involved in the initiation, progression and end-stage of CAVD remain largely unknown. The mechanisms of valve calcification in heart valves appear to be similar but not identical to those responsible for atherosclerosis [6]. This might be at least, in part, due to the specific nature and responses of valve interstitial and endothelial cells to different stimuli. Recent studies suggest that underlying mechanisms of CAVD are initiated at the endothelium leading to inflammation [7, 8]. Activation of inflammatory pathways is believed to promote cardiovascular calcification by the trans-differentiation of quiescent VICs into osteoblast-like VICs, forming calcific lesions which accumulate calcium phosphate mineral [7, 9, 10]. Mineral deposits have been shown in human valves [10, 11] and we recently demonstrated that calcium phosphate particles, composed of highly crystalline hydroxyapatite associated with 100% of calcific lesions and between 83%-100% in non-calcified regions are present in patients with CAVD [10, 12]. These particles were also detected in 80% of non-calcified aortic valve tissue from patients that had calcific lesions in another part of their cardiovascular system. An analysis of particle size showed a trend for increasing particle diameter with increasing disease severity [10]. Most surprisingly, these particles were found on 46% of aortic valves in which the cardiovascular system was apparently entirely free from calcific lesions. Spherical and semispherical deposits together with lamellar crystals have also been shown in calcified valves [13]. Immunolabelling of aortic valve tissues showed strong positive labelling for early osteoblastic transcription factors

RUNX2 and Sp7 expression in cells near the spherical particles but no osteocalcin. Additionally RUNX2 and Sp7 expression was observed in apparently healthy tissue with the presence of calcified particles. However, detection of these calcified particles does not by itself prove the hypothesis that these particles contribute to the pathogenesis of CAVD. Since these particles were present during all stages of CAVD, regardless of the presence of calcific lesions, it is suggested that these particles are the first mineralized structure formed and may play a fundamental role in calcific lesion formation and ultimately calcification. Despite this knowledge, the exact role of these particles in CAVD is still unknown.

The goal of the present study is to investigate the effects of these calcium phosphate particles on valvular cells. The calcium phosphate particles were isolated from human donor aortae and several concentrations of particles were studied in direct contact with a monoculture of VECs and VICs. Quantification of the particles was assessed by turbidity [14], scanning electron microscopy was used for characterization of the particles and cellular behaviour was studied with cell viability, proliferation and differentiation. It is hypothesized that these particles will stimulate a shift in phenotype of the cells into an activated and osteogenic phenotype that may progress the calcification process.

Material and methods

Human healthy aortae and calcified aortae were used for isolation of the particles. We have ascertained that these particles, whether isolated from valves or aortae, are identical in nature and healthy and diseased aortae were more readily available. 9 healthy aortae (mean age 42.1 years; range 4 days-65 years; SD=21.5; 6 females and 3 males) were obtained from heart valve donors, whose valves were judged unsuitable for clinical use or from explanted hearts of cardiac transplant recipients. The normal aortae were obtained from patients free from cardiovascular and valvular complications based on history, macroscopic and microscopic evaluation. These were unused aortae from healthy, heart donors, most of whom died from a cerebral haemorrhage due to head trauma with no underlying diseases. The aortic tissue was taken from adjacent to the aortic valves. Calcified aortic tissues, n=5,

were from heart donors or explanted hearts at the time of cardiac transplantation whose aortae showed visible evidence of calcification (mean age 66.3 years; range 54-78 years; SD=9.3; 2 female and 3 males). For cell isolation, healthy, aortic heart valves, n=7, were used (mean age 48 years; range 18-59 years; SD=15.0; 2 female and 5 males). These were also obtained from patients free from cardiovascular and valvular complications based on history, macroscopic and microscopic evaluation. These were unused valves mostly due to fenestrations from healthy, heart donors, most of whom died from a cerebral haemorrhage due to head trauma with no underlying diseases. The valves and aortae were not matched from donors. All human studies have been approved by the Brompton and Harefield trust ethics committee and Oxford Hospital. These studies have been performed in accordance with the ethical standards laid down in the 1964 Declaration of Helsinki and its later amendments. All donors gave their written informed consent prior to their inclusion in the study.

Cell isolation and culture

Healthy human valve leaflets were excised and washed in PBS once. The valve leaflets were incubated in a collagenase solution (Type A, 0.15% w/v; Roche, Life Sciences, United States) for 10 minutes at 37 °C under a forceful agitation to remove the VECs. The undigested tissue was removed, washed with PBS, minced, and incubated further for 3 hours in a fresh collagenase solution at 37 °C under forceful agitation to isolate the VICs. After centrifuging of the solution with the VECs, the resulting VEC pellets were plated out in gelatin coated tissue culture flasks. VECs were grown until confluent in endothelial media, defined as Endothelial Cell Growth Medium 2 (ECGM; PromoCell, Germany) containing 150 U/ml penicillin/streptomycin (P/S; Sigma Aldrich), 2 mM endothelial cell growth supplement, and 20% heat-inactivated fetal calf serum (FCS; Helena Biosciences, Sunderland, United Kingdom). The resulting VICs after centrifuging the other solution were grown until confluent in basic VIC media, defined as basal Dulbecco's Modified Eagle Medium (DMEM; Sigma Aldrich) containing 150 U/ml P/S, 2 mM L-Glutamine (L-Glut; Sigma Aldrich), and 10% FCS.

Once confluent, media is switched for fibroblast media, defined as basal DMEM containing 150 U/ml P/S, 2 mM L-Glut, 2% FCS, 5 µg/ml insulin (Sigma Aldrich), and 10 ng/ml fibroblast growth factor-2 (FGF2; Peprotech, United Kingdom) and cultured until further analysis.

Isolation of calcium phosphate particles

Healthy and diseased aortic tissues (1 cm by 1 cm), were excised and incubated overnight in a collagenase solution (2% w/v; Sigma Aldrich, Saint Louis, MO, United States) at 37 °C. After which, tissues were homogenized with a tissue grinder and again incubated overnight in the collagenase solution at 37 °C. After incubation, samples were centrifuged and washed three times with phosphate buffered saline (PBS; Sigma Aldrich). The resulting pellet was resuspended in 67% hydrazine solution (Sigma Aldrich) at 55 °C for 2 hours. Samples were centrifuged, washed once with deionized water and ethanol and stored dried in the freezer. Isolated particles from donors were not pooled.

Turbidity

For turbidity of the particles, isolated particles from all donors were suspended in 500 µl deionized water first. The particles were homogenized and mixed extensively by vortexing and the use of a pestle. The absorbance of the samples and dilutions were measured by using the Bio spectrophotometer plus (Eppendorf, New York, United States) at 600 nm, room temperature. For reproducibility, samples were measured immediately and after 5 days since the particles tend to sink.

Scanning electron microscopy/EDS/EDX

After quantification, samples of different particle donors were viewed for their histology with scanning electron microscopy. For chemical characterization, energy-dispersive X-ray spectroscopy (EDS/EDX) spectra were obtained from all samples and specific regions of interest.

Cell Viability, differentiation and proliferation

For cell experiments, these calcified particles were applied to a monoculture of VECs and VICs by adding them directly into the media and cell viability, proliferation and differentiation was analyzed. Cell viability was determined by fluorescent labelling with a LIVE/DEAD Viability kit for mammalian cells (Invitrogen, Life Technologies, United States) whereby particles from different donors (healthy and diseased; absorbance reading of 1.0 and 0.25, 10, 20, and 50 µl per 500 µl of media) were added to the cells and further cultured for a week. For apoptosis, cells were fixed after 7 days and stained with the In Situ Cell Death Detection Kit, Fluorescein [15].

Furthermore, the proliferation assay was carried out with a CellTiter 96 AQueous Non-Radioactive Cell Proliferation Assay kit (Promega, Madison, Wisconsin, United States).

To look at the potential of osteogenesis, differentiation was analysed by immunostainings and Western blotting. In short, both cell types were seeded, mono-cultured for three weeks with the particles added to the media (absorbance reading of 1.0, 20 µl per 500 µl of media) and analyzed for α-SMA, CD31, vWF, Vimentin (Dako), Collagen type I (Biologo), Collagen type III (Novotec), Osteocalcin (Abgent), SM-22 (Abcam), Osteopontin and CBFA-1 (R&D) by immunofluorescence and western blotting. Calcium deposits and mineralization was visualized by immunochemistry. More detailed methods can be found in the Supplemental Data.

Statistical analysis

Statistical analysis was performed using GraphPad Prism 5 (GraphPad Software, United States). Prior to analysis of significant differences, data was subjected to a Shapiro-Wilk normality test. Normal distributed data was subjected to a t-test or one-way ANOVA, followed by a Tukey post-hoc test. Other data was analyzed by a Kruskall Wallis nonparametric test. Differences were considered significant for $p < 0.05$. Data is presented as mean ± standard deviation. For the Westerns, data is presented as median ± standard deviation.

Results

Quantification of calcified particles

Absorbance values for the two time points from all samples showed good consistency/reproducibility (Figure 1A, 1B). Particles from the healthy donors (n=9) had a median absorbance of 1.47 (IQR= 0.33 – 2.14) compared to the significantly higher median absorbance of the diseased donors (n=5) of 2.96 (IQR= 1.88 – 5.64), p=0.04 (Figure 1C). The calcified particles from healthy donors showed a maximum absorbance of 2.7 and the diseased particles showed a minimum absorbance of 1.39. To determine effects of calcified particles from both the healthy and diseased donors an upper absorbance of 1.0 and a lower absorbance of 0.25 (by diluting the particles) were subsequently used as a high and low dose. Higher doses were deemed unsuitable considering the ratio of cells to particles and resulted in cell toxicity and death.

Scanning electron microscopy showed major diversity within the particles

A lot of variability in shape was seen in each sample (Figure 2A-B) with spherical and cubic formed particles. Furthermore, in each sample these different shapes and structures differed in size. The majority of the calcified particles were spherical in form with equal variation between the healthy and diseased donors.

Chemical composition of calcified particles

The majority of the particles, both spherical and cubic, revealed calcium (Ca), phosphorus (P) and smaller amounts of magnesium (Mg) (Figure 2C,D). However, in a small amount of particles, a small amount of carbon (C) and sodium (Na) was present (not shown).The percentage of phosphorus, oxygen, calcium, sodium and magnesium in the particles is depicted in Figure 2E. There were no differences in the composition of the particles for healthy and diseased donors.

Calcified particles increase vWF secretion in VECs

Control, healthy and untreated VECs expressed CD31 (red) and most VECs expressed weak expression of vWF (green) (Figure 3A). Treatment with calcified particles for 7 days, whereby particles were added in the media of healthy cells, showed no difference in staining of vWF and CD31 (not shown). For each treated group no expression of αSMA (red) and SM22 (green) was found (Figure 3A). No osteoblast markers were observed in VECs before and after 7 day treatment with the calcified particles (not shown). Only a very small percentage of the cells from one isolate in the positive control expressed α-SMA (red) and did not express α-SMA in the control samples. There was no difference between the groups treated with healthy and diseased aortae donors.

After 21 days, a higher percentage of cells were positive for CD31 (red) and co-expressed vWF (green) compared with the samples after one week after treatment with the positive control (Figure 3B). A higher number of cells demonstrated increased intensity of vWF and decreased intensity of CD31 staining in both calcified particle treated groups compared to the control. Expression of α-SMA (red) was seen in the positive control for one isolate while no cells were positive in the control. In this isolate, no α-SMA expressing endothelial cells were seen in calcified particle treated groups. No expression of SM22 was seen for each group or isolate. Weakly positive cells for osteopontin and no osteocalcin were found in treated groups, including the positive control.

Immunohistochemical staining showed no nodule formation after 3 weeks but some increase in alizarin red and ALP staining however osteogenic media (positive control) failed to induced any significant increase in these markers in VECs. No von Kossa positive staining was detected in any treated group after 21 days (Figure 4A). There was no difference between the groups treated with calcified particles from healthy and diseased aortae donors.

Calcified particles induce a change in phenotype of VICs

A 7 day treatment was not performed as this time was deemed insufficient for osteogenic changes. Vimentin was strongly expressed in all VICs in the control group and this

expression decreased in the positive control and treated groups after 21 days. No α-SMA was detected in the control group and positive control. In contrast, α-SMA positive cells can be seen in the healthy and diseased aortae donor groups (Figure 5). Furthermore, intensities of α-SMA expression varied in these groups indicating different degrees of differentiation of the VIC phenotype. Control cells expressed no osteopontin, osteocalcin or collagen I with baseline expression of collagen III. The positive control showed no increase in osteopontin or osteocalcin but there was a very slight increase in expression of collagen I and III. The calcified particle treated groups showed very weak expression of osteopontin and osteocalcin and moderate expression of collagen I and III (Figure 5).

Alizarin Red and ALP staining of VICs (Figure 4) showed positive staining in over 30% of VICs and von Kossa staining showed positive staining in over 10% of VICs when treated with the calcified particles but these stains were negative for the control and positive control. There was no difference between the groups treated with calcified particles from healthy and diseased aortae donors.

Calcified particles induce myofibroblastic and osteoblastic changes

For the calcified particle treated VECs, there was a significant 1.78-fold decrease in the expression of VE-CAD p=0.04; a significant 3.05-fold decrease in CD31, p=0.009; a significant 1.56-fold increase in vWF, p=0.02; no change in α-SMA, p=0.82 and no change in osteopontin, p=0.35, (Figure 6). The collagen antibodies did not work on Westerns, CBFA-1 and osteocalcin were not detected in VECs before or after treatment. There was no difference between the healthy and diseased calcified particle treated groups.

For the VICs treated with calcified particles, there was a significant 2.70-fold increase in the expression of α-SMA, p=0.03; a significant 3.48-fold increase in the expression of osteopontin, p=0.01 and there was no change in the expression of CBFA-1, p=0.93, (Figure 6). There was no difference between the groups treated with calcified particles from healthy and diseased aortae donors.

Cell viability is reduced for high concentrations of particles

Overall, VEC viability remained high after treatment for 7 days (> 80%) using the lower volumes of 10 and 20 µl of [0.25] and 10 µl of [1.0]. However, for the highest dose of particles (absorbance reading of 1.0, 20 and 50 µl per 500 µl of media) VECS were significantly less viable compared to the control (93.83 ± 4.7 % vs 65.38 ± 24.68 %, $p < 0.05$) (Figure 7A, 7C). There was no difference between the groups treated with calcified particles from healthy and diseased aortae donors.

VICs were significantly less viable compared to the control (93.43 ± 9.0 %) when treated with the lower dose of calcified particles (absorbance reading of 0.25, 10µl per 500µl of media (84.57 ± 11.5 %) and 20 µl per 500 µl (79.4 ± 16.4 %), $p < 0.05$). For the highest doses of calcified particles (absorbance reading of 1.0, 20 µl per 500 µl and 50 µl per 500 µl of media) VICS were significantly less viable compared to the control (93.43 ± 9.0 % vs 79.9 ± 18.3 % and 93.43 ± 9.0 % vs 54.6 ± 22.3 %, $p < 0.05$) (Figure 7A, 7C). Furthermore, no differences between healthy and diseased aortae particle treated groups were seen.

The calcified particle treated groups showed a significantly increased number of TUNEL positive VECs 15.8% ± 16.0% compared to control = 2.0±3.7%, p=0.005 and VICs, 4.0% ± 4.4% showed no difference in TUNEL positivity compared to control = 3.1% ± 4.3% (Figure 8A and B). However, it was noted that there were fewer cells present for the treated groups compared with both controls.

Proliferative capacity is unchanged by addition of calcified particles

Proliferative capacity for VECs was not changed for the groups with particles compared with the control after 7 and 14 days (Figure 8C and 8D respectively). Proliferative capacity for VICs was unchanged after 7 and 14 days (Figure 8E and 8F respectively) however the diseased [0.25] group had a higher proliferative capacity compared with the control after 14 days (supplement Figure 1) (p=0.0132). For VECs, there was no difference between the healthy and diseased donor groups. The positive control was significantly higher compared to all groups due to the increased concentration of growth factors.

Discussion

This study has demonstrated that calcified particles isolated from healthy and diseased aortic donors have the capacity of inducing phenotypic and pathological remodelling of human VECs and VICs as well as affecting viability and inducing apoptosis in VECs.

Turbidity was able to gauge a measure of the particles and this was reproducible and consistent over different days and has been used with other calcified particles [14, 16]. Therefore, these optical density readings were used as indicator of the concentration and enabled consistent dosing between samples. A lower range of particle concentration was used that encompassed the range from the healthy donors at a lower concentration of particles (absorbance reading of 0.25; [0.25]) and a higher concentration (absorbance reading of 1.0; [1.0]) representing diseased donors. The particles had a high variability, differing in shape (spherical and cubic) and size (100 nm to 3.5 μm). No differences in composition of the particles were found between the healthy and diseased donors however the amount of calcified particles in the diseased donors was significantly increased and this has been shown to be greatly increased in diseased valves and aortae [10]. The heterogeneity in the calcified particles has been linked to the physicochemical parameters of their native growth niche and to the local condition of the extracellular matrix [13].

Using SEM and energy dispersive x-ray spectroscopy, the isolated calcified particles demonstrated identical size, shape distribution and spectra to the in vivo detected calcified particles. Elemental analysis of isolated calcified particles demonstrated peaks for calcium, phosphorus, oxygen and magnesium as detected for the in vivo particles [10]. Though this elemental composition is similar to that of bone [17], it was shown that surface area electron diffraction patterns of the in vivo calcified particles were typical of highly crystalline hydroxyapatite whereas bone consists of a poorly crystalline apatite [10, 17, 18]. The origin of these calcified particles is the subject of ongoing research and they could arise due to a number of different cellular mechanisms and from a number of different cells. A variety of bodies are released from cells such as apoptotic bodies, exosomes, matrix vesicles, extracellular vesicles and microparticles and there is significant overlap in their size and

structure[19, 20]. The size range of these calcified particles is considerably larger, ranging from 100 nm up to 2.5 μm in diameter (data from these current samples and from [10]), compared to that of extracellular vesicles released from smooth muscle cells in normal and calcifying media which was shown to be between 30 and 300nm [21]. This lower range also holds true for exosomes, matrix vesicles and microparticles [22]. The larger size of these calcified particles may arise due to extracellular nucleation of hydroxyapatite through the deposition of Ca^{2+} and P_i in the hole zone regions of collagen fibrils within the matrix [23]. As these calcified particles represent a novel subparticle population in valves and aortae, further research is aimed at identifying key cell surface markers and to enable the identification of the cellular origin. Elevated levels of extracellular calcium has been shown to induce mineralization of vascular smooth muscle cell-derived matrix vesicles [24] and both smooth muscle cells [25] and matrix vesicles [26] have been demonstrated in calcified valves.

Particles from both healthy and diseased donors significantly increased the expression of vWF in VECs and significantly decreased CD31 and VE-cadherin after 21 days incubation. In general, vWF plays a key role in haemostasis by recruiting platelets to sites of vascular damage [27]. A higher expression of vWF might be an early sign of endothelial activation [28] and is related to endothelial damage [27, 29]. Calcium phosphate particles were shown to stimulate IL-8 expression and NF-κB activity in human gingival epithelial cells, which are both involved in the process of inflammation [30]. Endothelial damage and dysfunction is thought to be the initiating factor modulated by circulating inflammatory cells, proteins and cyclic strain in the process of calcification and further studies will aim to identify early indicators of inflammation such as NFκB, adhesion molecules and cytokines after treatment with calcified particles. VECs treated with calcified particles showed no evidence of endothelial to mesenchymal (EMT) or osteogenic transformation over 21 days as evidenced from the data in this study. This suggests that these human VEC isolates, compared to VICs, are more resistant to a change in their phenotype when exposed to these calcified particles. One VEC isolate was able to undergo EMT when treated with TGFβ1 and TGFβ1 is a key initiator for EMT [31]. There was no detectable osteocalcin or CBFA-1, no increase in

osteopontin and no nodules, ALP positive cells or calcium deposits were found when VECs were treated with calcified particles. Additionally human VEC isolates did not undergo osteogenic differentiation when treated with osteogenic medium which contrasts to clonal populations of ovine VECs [32] which were shown to undergo osteogenic differentiation using standard osteogenic protocols. This difference may be related to species, age, gender [33] and definitely to isolate type.

The treatment of VICs for 21 days with the particles showed an increase in myofibroblastic and osteoblastic differentiation by immuno- and histochemical staining. β-tricalcium phosphate crystallized micron particles, which resemble the calcified particles used in this study, have been shown to enhance calcification of human mesenchymal stem cells in vitro and decrease cell viability [34]. Porcine VICs have been compared with osteoblastic cell types at different stages of differentiation and it has been suggested that VICs may not need to progress through an activated myofibroblastic stage before reaching an osteoblast-like phenotype [35]. However, it has been shown that there is a relationship between myofibroblastic porcine VIC activity and initial calcific nodule formation [36] and that differentiation of VICs to myofibroblasts was a key mechanistic step in the process of early mineralization [37]. Nodules were not detected at any stage of our experiments, with or without calcified particles or osteogenic media. Crucially, it must be noted that in the present study VICs from humans that are fibroblastic in nature [38] and of an older age were used and this may have slowed their rate of differentiation while other studies used animal VICs of a younger age which normally are activated in vitro and may have a higher differentiation potential. Further research of the calcified particles with VICs will include short term analysis for phenotypic changes to see whether VICs progress through an activated phenotype before differentiation into an osteoblast-like VIC and to assess early markers of activation and cell signalling.

Differentiation of VECs and VICs was assessed separately in this study however there is cross-talk between these two cell types and they are able to modulate each other's

behaviour. VICs were shown to inhibit osteogenic differentiation and endothelial to mesenchymal transformation of VECs [39, 40]. Additionally VECs were able to reverse VIC activation [40]. A co-culture model would elucidate this cross-talk and enable a better understanding of the time course, the differentiation capacity of the calcified particles and the differentiation potential of the cells. The calcified particles were in direct contact with most of the cells and whether they are able to modulate valvular cells without being in direct contact, using transwells, warrants investigation. Also there may be synergistic effects with mechanical loading which could affect valvular behaviour hence co-culture under physiological haemodynamic loading should be performed. SEM was used to assess contact between the cells and the calcified particles and showed some embedding of the particles within the cell membranes, possibly due to their size and sedimentation (Supplemental Figure 2). However, this was complicated by other cellular membrane-bound structures and debris and engulfment of the calcified particles by the valvular cells cannot be confirmed as yet. Further studies using TEM are ongoing and labelling of these particles would give more insight into their mechanisms and roles in the pathogenesis of calcification.

VEC viability was significantly decreased by 65% for the highest dose of healthy particles. Those from diseased donors also showed a decrease but this did not reach significance, probably due to the limited time period of the experiment. In the treated groups only a few apoptotic cells can be seen while 50% of dead cells were seen in the cell viability staining. This may suggest that both donors mainly cause necrosis instead of apoptosis at high doses. However, a lower percentage of cells were present in the treated groups compared with the control implying that dead cells were washed away or already had undergone apoptosis. Therefore, a time course with different concentrations of each donor needs to be performed in order to distinguish better between apoptosis and necrosis. No differences in proliferative capacity were seen for VECs with these concentrations for both donor groups.

VICs treated with a high concentration of healthy donor particles demonstrated significant cell death. The highest concentration for the diseased donor group, although lower than

control, showed no significant difference compared with the control and this may be due to the short time period. The TUNEL staining showed a similar pattern for VECs. Apoptosis has been documented in human calcified valves [41, 42] and was shown to be mediated through the pro-apoptotic cytokines TRAIL [41] and TGFβ1 [42]. Apoptosis has been thought to lead to growth of calcium phosphate crystal structures exacerbating the calcification process [43]. Although the proliferative capacity for VICs was not affected by the particles after 7 days, a significant increase for the low dose of particles from the diseased donor (absorbance reading of 0.25, 10 µl per 500 µl) was seen after 14 days. This could mean that these VICs become more activated and thus proliferate more. However, proliferation was not seen for the high concentration (absorbance reading of 1.0), suggesting this might be causing cell death.

Differences between the effect of the calcified particles on cell viability and proliferation for VECs and VICs may be due to the differences in size or native of the two cell types. VECs are much smaller than VICs, meaning that a smaller surface area is available to interact with the particles compared with the larger VICs. This could have led to a higher VEC viability and could explain the lack of changes in proliferation and osteogenic differentiation. Differences in physicochemical characteristics of the particles may have a different effect on valvular cells leading to a different contribution to calcification. Furthermore, apatite is not toxic to human cells in bones and teeth and used in several in vivo applications [44]. However, it may cause opposite effects in other tissues. Labelling of the different particle structures and investigating their effects would be very important and could give insights into the location and mechanisms of interaction with the cells since it was not possible to visualize them with SEM and check for ingestion (data not shown).

In conclusion, this study demonstrates that calcified particles isolated from human aortae, used at these doses, have pathological significance in that they are able to activate a high percentage of human VECs within 21 days. Calcified particles were able to activate a subset of VICs to the myofibroblastic and osteoblastic phenotype. The particles also have a

significant effect on the viability of both VECs and VICs signifying their clinical importance. Further work is warranted investigating the signalling mechanisms involved.

Acknowledgements

We would like to thank the Royal Brompton valve biobank for the procurement of normal valves and the Oxford hospital for the aortic tissues. The authors declare that they have no conflict of interest.

Funding

The authors would like to thank the Magdi Yacoub Institute for funding this research.

Disclosure.

Nothing to disclose.

References

1. Speer MY and Giachelli CM. Regulation of cardiovascular calcification. *Cardiovasc Pathol*. 2004;13:63-70.
2. Freeman RV and Otto CM. Spectrum of calcific aortic valve disease: pathogenesis, disease progression, and treatment strategies. *Circulation*. 2005;111:3316-26.
3. Otto CM, Lind BK, Kitzman DW, Gersh BJ and Siscovick DS. Association of aortic-valve sclerosis with cardiovascular mortality and morbidity in the elderly. *N Engl J Med*. 1999;341:142-7.
4. Aronow WS, Ahn C, Shirani J and Kronzon I. Comparison of frequency of new coronary events in older subjects with and without valvular aortic sclerosis. *Am J Cardiol*. 1999;83:599-600, A8.
5. Stewart BF, Siscovick D, Lind BK, Gardin JM, Gottdiener JS, Smith VE, Kitzman DW and Otto CM. Clinical factors associated with calcific aortic valve disease. Cardiovascular Health Study. *J Am Coll Cardiol*. 1997;29:630-4.
6. Xu S, Liu AC and Gotlieb AI. Common pathogenic features of atherosclerosis and calcific aortic stenosis: role of transforming growth factor-beta. *Cardiovasc Pathol*. 2010;19:236-47.
7. Hjortnaes J, New SE and Aikawa E. Visualizing novel concepts of cardiovascular calcification. *Trends Cardiovasc Med*. 2013;23:71-9.
8. Aikawa E, Nahrendorf M, Sosnovik D, Lok VM, Jaffer FA, Aikawa M and Weissleder R. Multimodality molecular imaging identifies proteolytic and osteogenic activities in early aortic valve disease. *Circulation*. 2007;115:377-86.
9. Anderson HC. Matrix vesicles and calcification. *Curr Rheumatol Rep*. 2003;5:222-6.
10. Bertazzo S, Gentleman E, Cloyd KL, Chester AH, Yacoub MH and Stevens MM. Nano-analytical electron microscopy reveals fundamental insights into human cardiovascular tissue calcification. *Nat Mater*. 2013;12:576-83.

11. Orzechowska S, Wrobel A, Goncerz G, Podolec P and Rokita E. Physicochemical and micro-tomographic characterization of inorganic deposits associated with aortic stenosis. *J Heart Valve Dis*. 2014;23:40-7.
12. Bertazzo S, Steele JA, Chester AH, Yacoub MH and Stevens MM. Cardiovascular calcification violet pearl. *Lancet*. 2014;384:1294.
13. Cottignoli V, Relucenti M, Agrosi G, Cavarretta E, Familiari G, Salvador L and Maras A. Biological Niches within Human Calcified Aortic Valves: Towards Understanding of the Pathological Biomineralization Process. *Biomed Res Int*. 2015;2015:542687.
14. Kajander EO and Ciftcioglu N. Nanobacteria: an alternative mechanism for pathogenic intra- and extracellular calcification and stone formation. *Proc Natl Acad Sci U S A*. 1998;95:8274-9.
15. Messika-Zeitoun D, Detaint D, Leye M, Tribouilloy C, Michelena HI, Pislaru S, Brochet E, Iung B, Vahanian A and Enriquez-Sarano M. Comparison of semiquantitative and quantitative assessment of severity of aortic regurgitation: clinical implications. *J Am Soc Echocardiogr*. 2011;24:1246-52.
16. Ciftcioglu N, Miller-Hjelle MA, Hjelle JT and Kajander EO. Inhibition of nanobacteria by antimicrobial drugs as measured by a modified microdilution method. *Antimicrob Agents Chemother*. 2002;46:2077-86.
17. Rey C, Combes C, Drouet C and Glimcher MJ. Bone mineral: update on chemical composition and structure. *Osteoporos Int*. 2009;20:1013-21.
18. Nudelman F, Pieterse K, George A, Bomans PH, Friedrich H, Brylka LJ, Hilbers PA, de With G and Sommerdijk NA. The role of collagen in bone apatite formation in the presence of hydroxyapatite nucleation inhibitors. *Nat Mater*. 2010;9:1004-9.
19. Bobrie A, Colombo M, Krumeich S, Raposo G and Thery C. Diverse subpopulations of vesicles secreted by different intracellular mechanisms are present in exosome preparations obtained by differential ultracentrifugation. *J Extracell Vesicles*. 2012;1.
20. Aikawa E. Extracellular vesicles in cardiovascular disease: focus on vascular calcification. *J Physiol*. 2016;594:2877-80.
21. Hutcheson JD, Goettsch C, Pham T, Iwashita M, Aikawa M, Singh SA and Aikawa E. Enrichment of calcifying extracellular vesicles using density-based ultracentrifugation protocol. *J Extracell Vesicles*. 2014;3:25129.
22. Gyorgy B, Szabo TG, Pasztoi M, Pal Z, Misjak P, Aradi B, Laszlo V, Pallinger E, Pap E, Kittel A, Nagy G, Falus A and Buzas EI. Membrane vesicles, current state-of-the-art: emerging role of extracellular vesicles. *Cell Mol Life Sci*. 2011;68:2667-88.
23. Landis WJ and Jacquet R. Association of calcium and phosphate ions with collagen in the mineralization of vertebrate tissues. *Calcif Tissue Int*. 2013;93:329-37.
24. Kapustin AN, Davies JD, Reynolds JL, McNair R, Jones GT, Sidibe A, Schurgers LJ, Skepper JN, Proudfoot D, Mayr M and Shanahan CM. Calcium regulates key components of vascular smooth muscle cell-derived matrix vesicles to enhance mineralization. *Circ Res*. 2011;109:e1-12.
25. Latif N, Sarathchandra P, Chester AH and Yacoub MH. Expression of smooth muscle cell markers and co-activators in calcified aortic valves. *Eur Heart J*. 2015;36:1335-45.
26. Kim KM. Calcification of matrix vesicles in human aortic valve and aortic media. *Fed Proc*. 1976;35:156-62.
27. Nightingale T and Cutler D. The secretion of von Willebrand factor from endothelial cells; an increasingly complicated story. *J Thromb Haemost*. 2013;11 Suppl 1:192-201.
28. Zanetta L, Marcus SG, Vasile J, Dobryansky M, Cohen H, Eng K, Shamamian P and Mignatti P. Expression of Von Willebrand factor, an endothelial cell marker, is up-regulated by angiogenesis factors: a potential method for objective assessment of tumor angiogenesis. *Int J Cancer*. 2000;85:281-8.
29. Mannucci PM. von Willebrand factor: a marker of endothelial damage? *Arterioscler Thromb Vasc Biol*. 1998;18:1359-62.

30. Sakai Y, Nemoto E, Kanaya S, Shimonishi M and Shimauchi H. Calcium phosphate particles induce interleukin-8 expression in a human gingival epithelial cell line via the nuclear factor-kappaB signaling pathway. *J Periodontol*. 2014;85:1464-73.
31. Paranya G, Vineberg S, Dvorin E, Kaushal S, Roth SJ, Rabkin E, Schoen FJ and Bischoff J. Aortic valve endothelial cells undergo transforming growth factor-beta-mediated and non-transforming growth factor-beta-mediated transdifferentiation in vitro. *Am J Pathol*. 2001;159:1335-43.
32. Wylie-Sears J, Aikawa E, Levine RA, Yang JH and Bischoff J. Mitral valve endothelial cells with osteogenic differentiation potential. *Arterioscler Thromb Vasc Biol*. 2011;31:598-607.
33. McCoy CM, Nicholas DQ and Masters KS. Sex-related differences in gene expression by porcine aortic valvular interstitial cells. *PLoS One*. 2012;7:e39980.
34. Nakagawa Y, Muneta T, Tsuji K, Ichinose S, Hakamatsuka Y, Koga H and Sekiya I. β-Tricalcium Phosphate Micron Particles Enhance Calcification of Human Mesenchymal Stem Cells In Vitro. *Journal of Nanomaterials*. 2013;2013:13.
35. Monzack EL and Masters KS. Can valvular interstitial cells become true osteoblasts? A side-by-side comparison. *J Heart Valve Dis*. 2011;20:449-63.
36. Benton JA, Kern HB, Leinwand LA, Mariner PD and Anseth KS. Statins block calcific nodule formation of valvular interstitial cells by inhibiting alpha-smooth muscle actin expression. *Arterioscler Thromb Vasc Biol*. 2009;29:1950-7.
37. Hjortnaes J, Goettsch C, Hutcheson JD, Camci-Unal G, Lax L, Scherer K, Body S, Schoen FJ, Kluin J, Khademhosseini A and Aikawa E. Simulation of early calcific aortic valve disease in a 3D platform: A role for myofibroblast differentiation. *J Mol Cell Cardiol*. 2016.
38. Latif N, Quillon A, Sarathchandra P, McCormack A, Lozanoski A, Yacoub MH and Chester AH. Modulation of human valve interstitial cell phenotype and function using a fibroblast growth factor 2 formulation. *PLoS One*. 2015;10:e0127844.
39. Hjortnaes J, Shapero K, Goettsch C, Hutcheson JD, Keegan J, Kluin J, Mayer JE, Bischoff J and Aikawa E. Valvular interstitial cells suppress calcification of valvular endothelial cells. *Atherosclerosis*. 2015;242:251-60.
40. Shapero K, Wylie-Sears J, Levine RA, Mayer JE, Jr. and Bischoff J. Reciprocal interactions between mitral valve endothelial and interstitial cells reduce endothelial-to-mesenchymal transition and myofibroblastic activation. *J Mol Cell Cardiol*. 2015;80:175-85.
41. Galeone A, Brunetti G, Oranger A, Greco G, Di Benedetto A, Mori G, Colucci S, Zallone A, Paparella D and Grano M. Aortic valvular interstitial cells apoptosis and calcification are mediated by TNF-related apoptosis-inducing ligand. *Int J Cardiol*. 2013;169:296-304.
42. Jian B, Narula N, Li QY, Mohler ER, 3rd and Levy RJ. Progression of aortic valve stenosis: TGF-beta1 is present in calcified aortic valve cusps and promotes aortic valve interstitial cell calcification via apoptosis. *Ann Thorac Surg*. 2003;75:457-65; discussion 465-6.
43. Hutcheson JD, Venkataraman R, Baudenbacher FJ and Merryman WD. Intracellular Ca(2+) accumulation is strain-dependent and correlates with apoptosis in aortic valve fibroblasts. *J Biomech*. 2012;45:888-94.
44. Ciftcioglu N and McKay DS. Pathological calcification and replicating calcifying-nanoparticles: general approach and correlation. *Pediatr Res*. 2010;67:490-9.

Figures

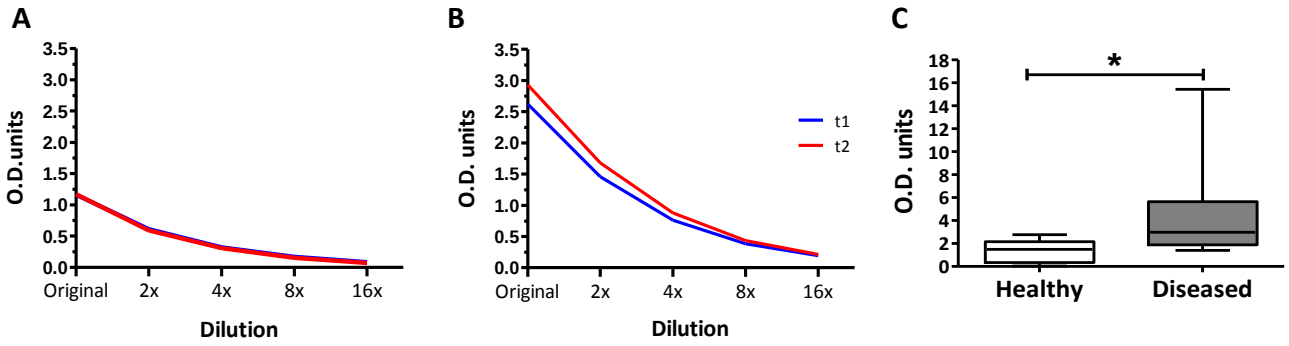

Figure 1. Turbidity measurements of a healthy donor (A), a diseased donor (B) at t1, directly after preparation and t2, after 5 days for several dilutions of each donor sample and graph showing median O.D.s and IQR for both groups (C). *p<0.05

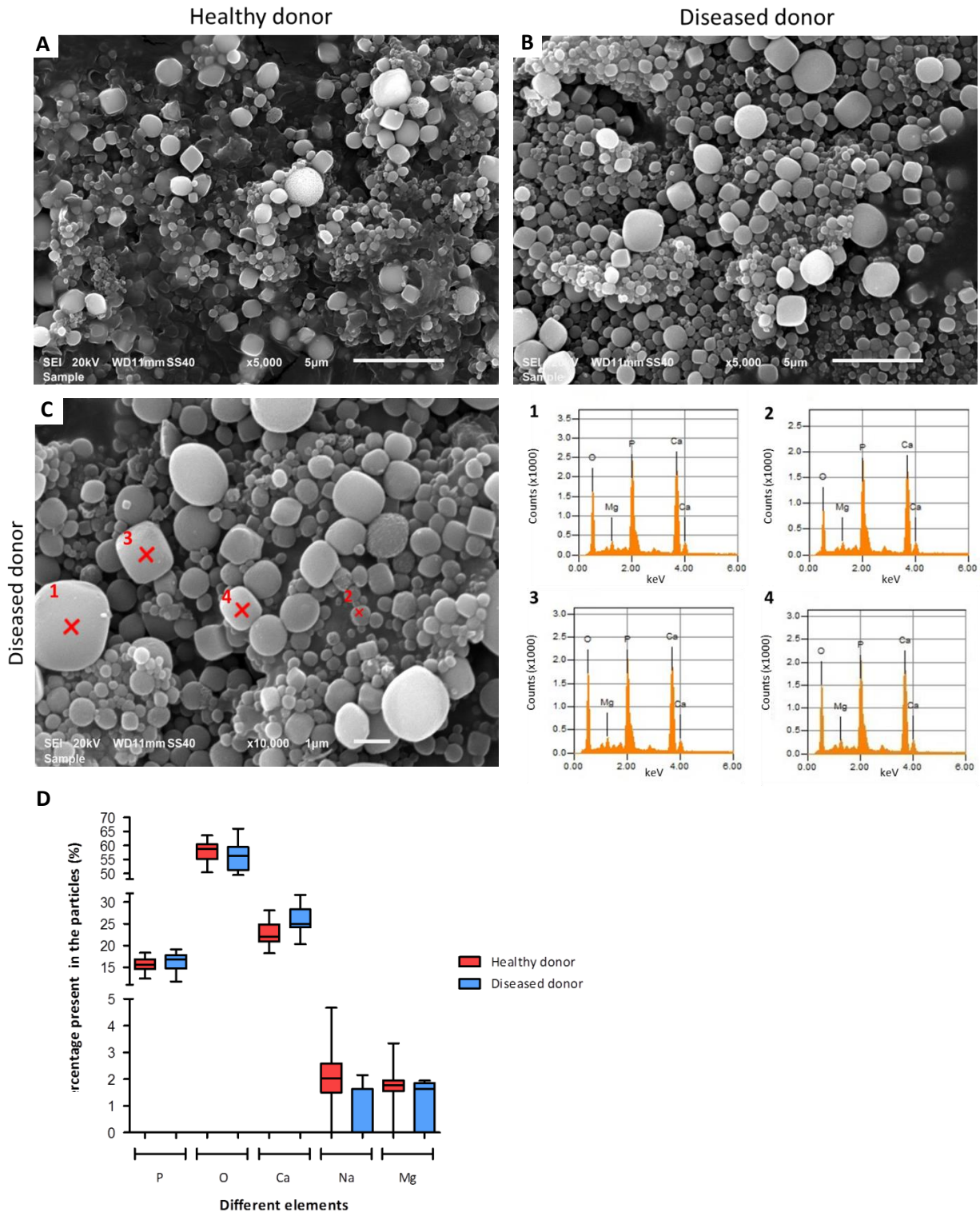

Figure 2. Representative SEM micrographs of the spherical particles isolated from a healthy (A) and a diseased donor (B). Higher magnification SEM micrograph of the spherical particles (C) with elemental analysis of different spherical particles in size and structure can be seen (1=big spherical particle, 2=small spherical particle, 3=big cubic particle and 4=small cubic particle). The representative corresponding EDS spectra were collected at the numbered sites indicated with a cross on micrographs. Mean percentage of phosphorus (P),

oxygen (O), calcium ^{37}, sodium (Na) and magnesium (Mg) of the different particles for healthy (red) and diseased donors (blue) (D). Scale bars indicate 5 µm in A and B; 1µm in C.

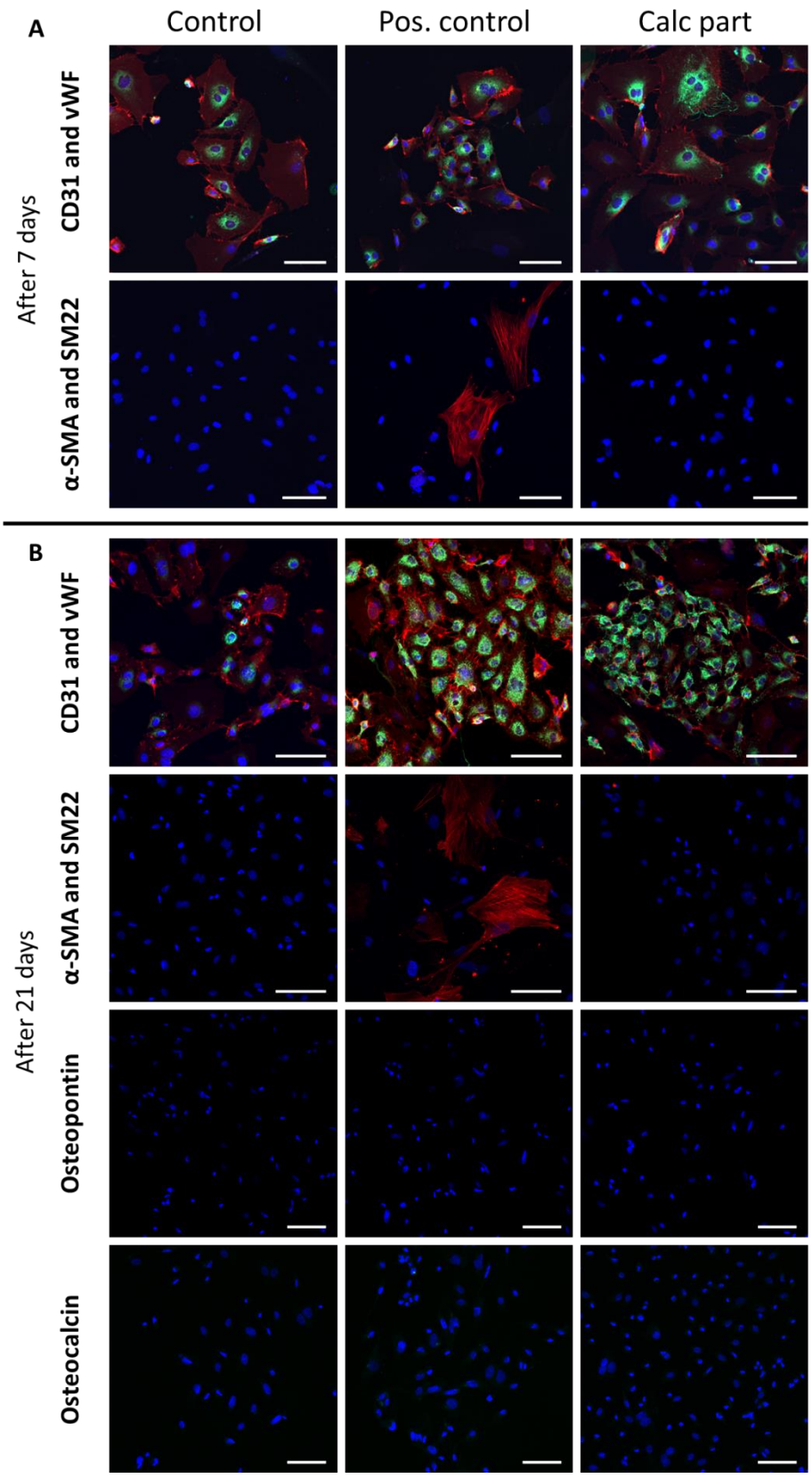

Figure 3. Immunostaining of VECs after 7 days of culturing (A). Data labelled as control are untreated VECs and the positive control is from VECs cultured with TGF-β1. VECs are

double stained for CD31 (red) and vWF (green) and double stained for α-SMA (red) and SM22 (green). Immunostaining of cultured VECs with calcified particles, labelled as calc part, after 21 days (B). Data labelled as positive control is from VECs cultured with osteogenic media. VECs are double stained for CD31 (red) and vWF (green), α-SMA (red) and SM22 (green), and for osteopontin (red) and osteocalcin (red). Scalebars represent 50 µm.

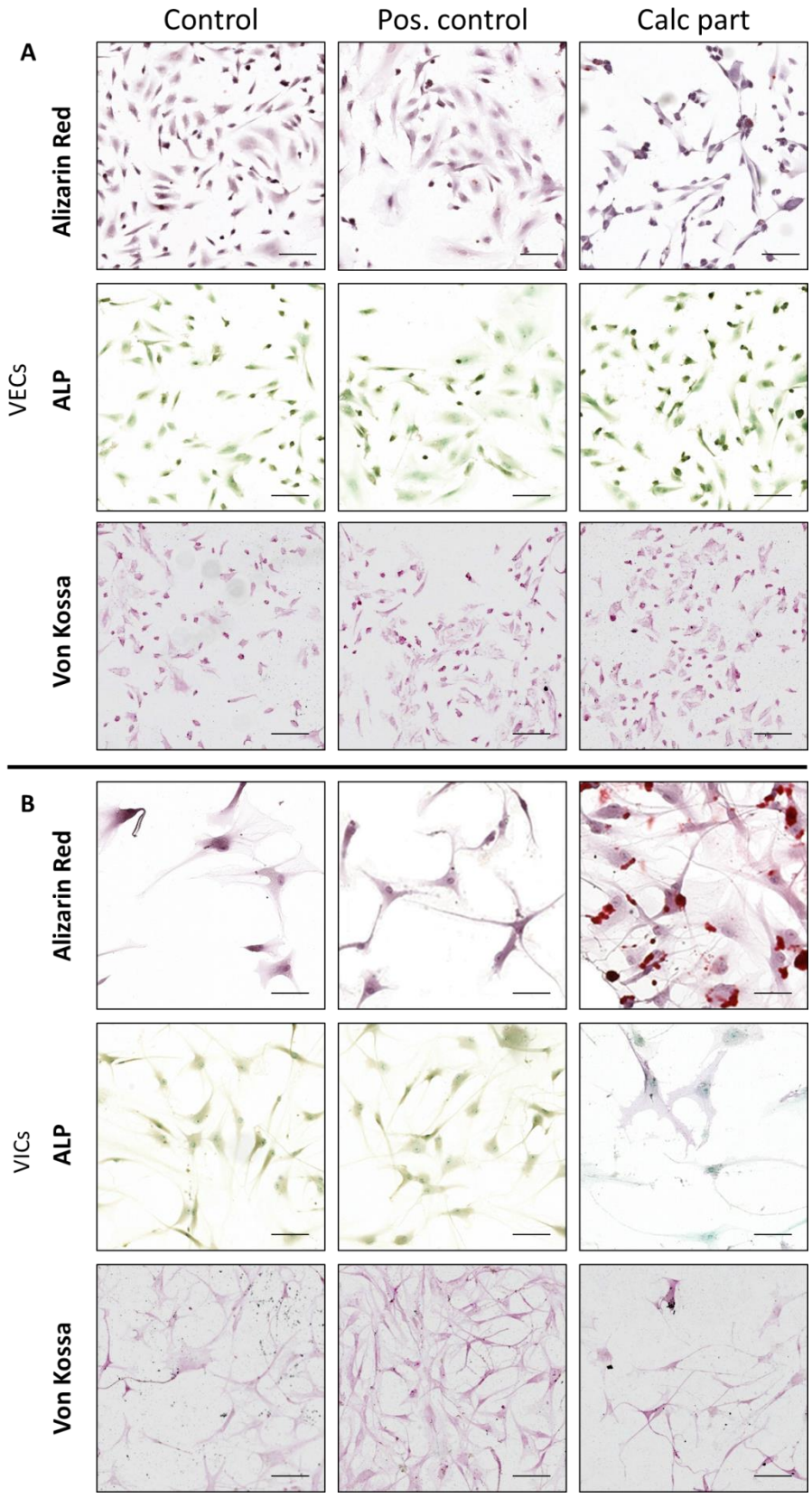

Figure 4. Immunochemical staining of VECs (A) and VICs (B) after 21 days of culturing with two different donors of particles (calc part) stained for Alizarin Red, ALP and with von Kossa.

Light green and van Gieson were used as counterstaining (green and pink, respectively). Data labelled as positive control is from cells cultured with osteogenic media and the control is without treatment of the particles. Scalebars represent 100 µm.

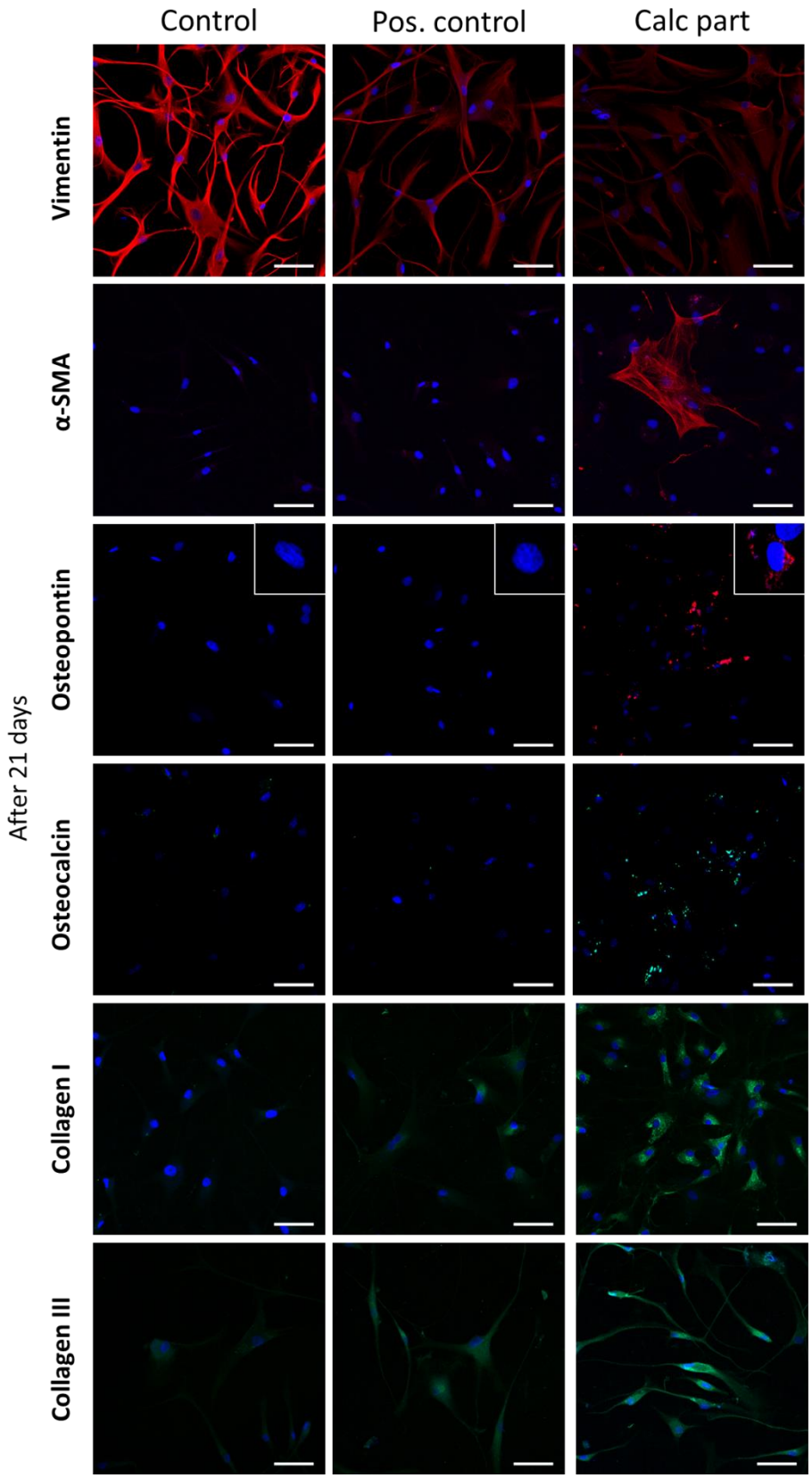

Figure 5. Immunostaining of VICs after 21 days of culturing with calcified particles. Data labelled as control is without treatment and the positive control is from VICs cultured with

osteogenic media. Coverslips are stained for vimentin (red), α-SMA (red), osteopontin (red), osteocalcin (green), collagen type I (green), and collagen type III (green). Scalebars represent 50 µm, inserts for osteopontin show higher magnification.

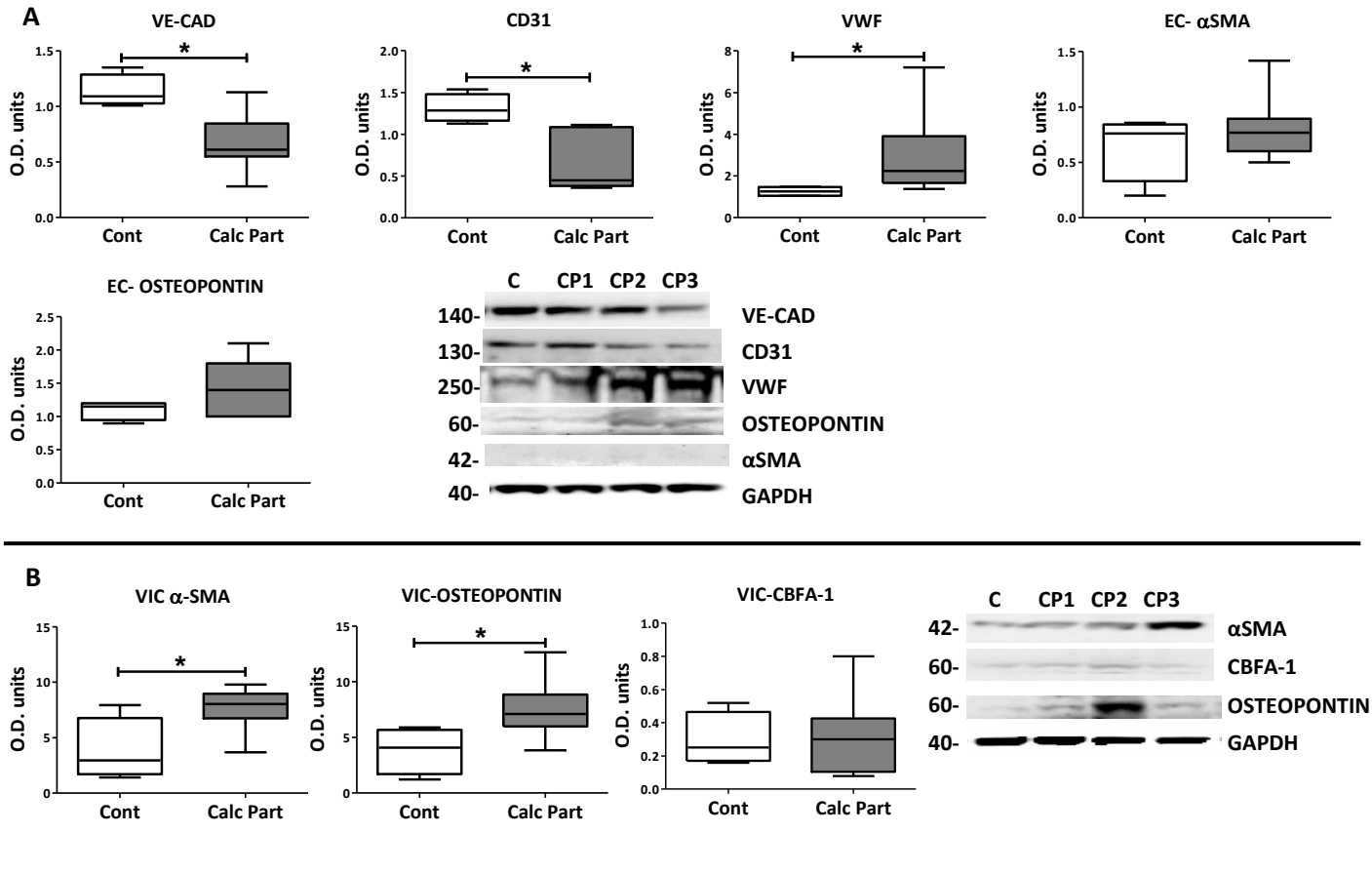

Figure 6. Graphs showing quantitative Western data of VECs (A) and VICs (B) treated with control (Cont; C) and calcified particles (Calc part; CP1, CP2 and CP3). Graphs show median and interquartile ranges. * $p<0.05$

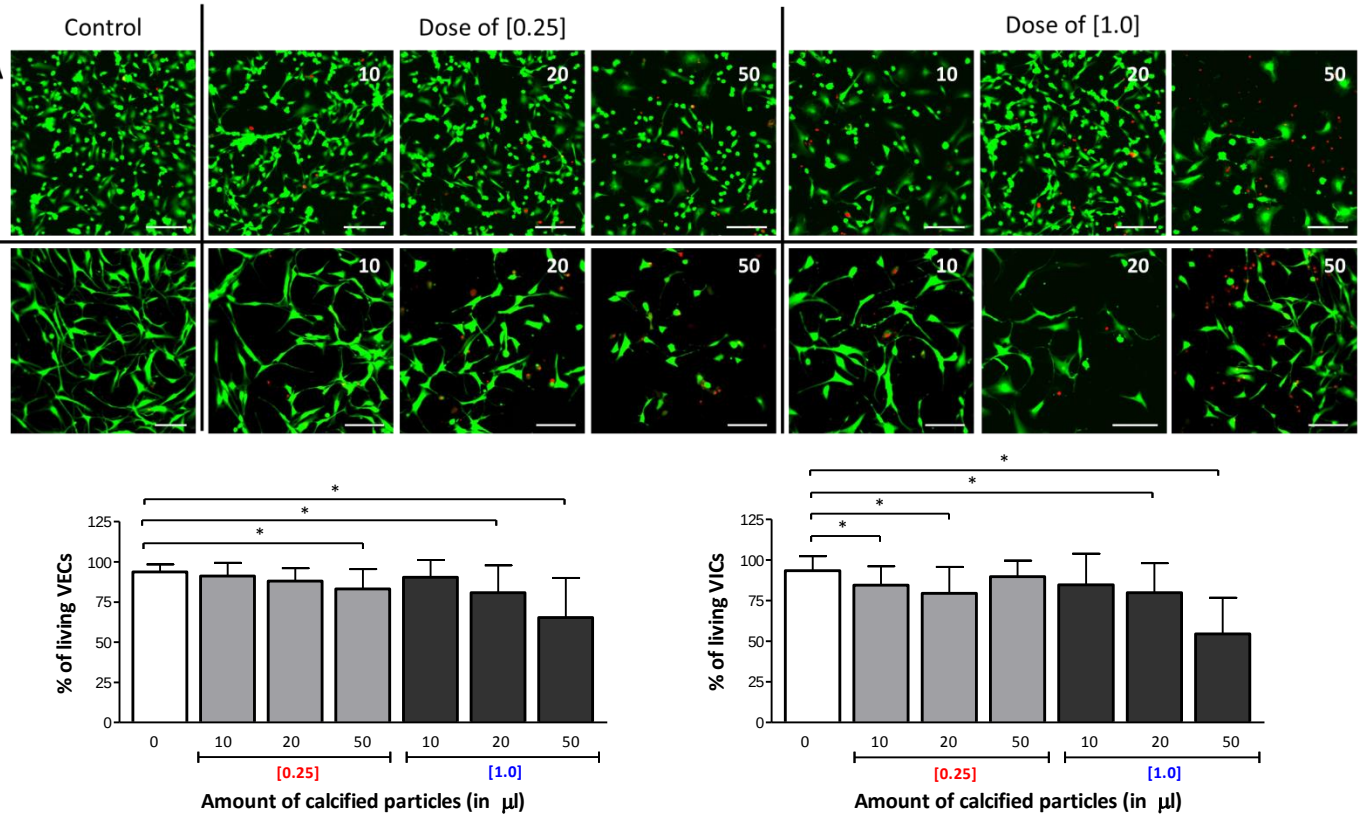

Figure 7. Cell viability of VECs (A) and VICs (B) with different amounts of particles from healthy and diseased donors after 7 days. For both cell types, several volumes of the particles are added; 10, 20, and 50 µl per 500 µl media of the ODs 0.25 and 1.0. Green represent living cells, red represent dead cells and the control did not receive any treatment. Quantification of the percentage of living VECs (C) and VICs (D) as determined from the images with MATLAB for healthy and diseased donors. VECs are considerably smaller in size than VICs. Scale bars, 100 µm. Data are depicted as mean and SD. * $p < 0.05$.

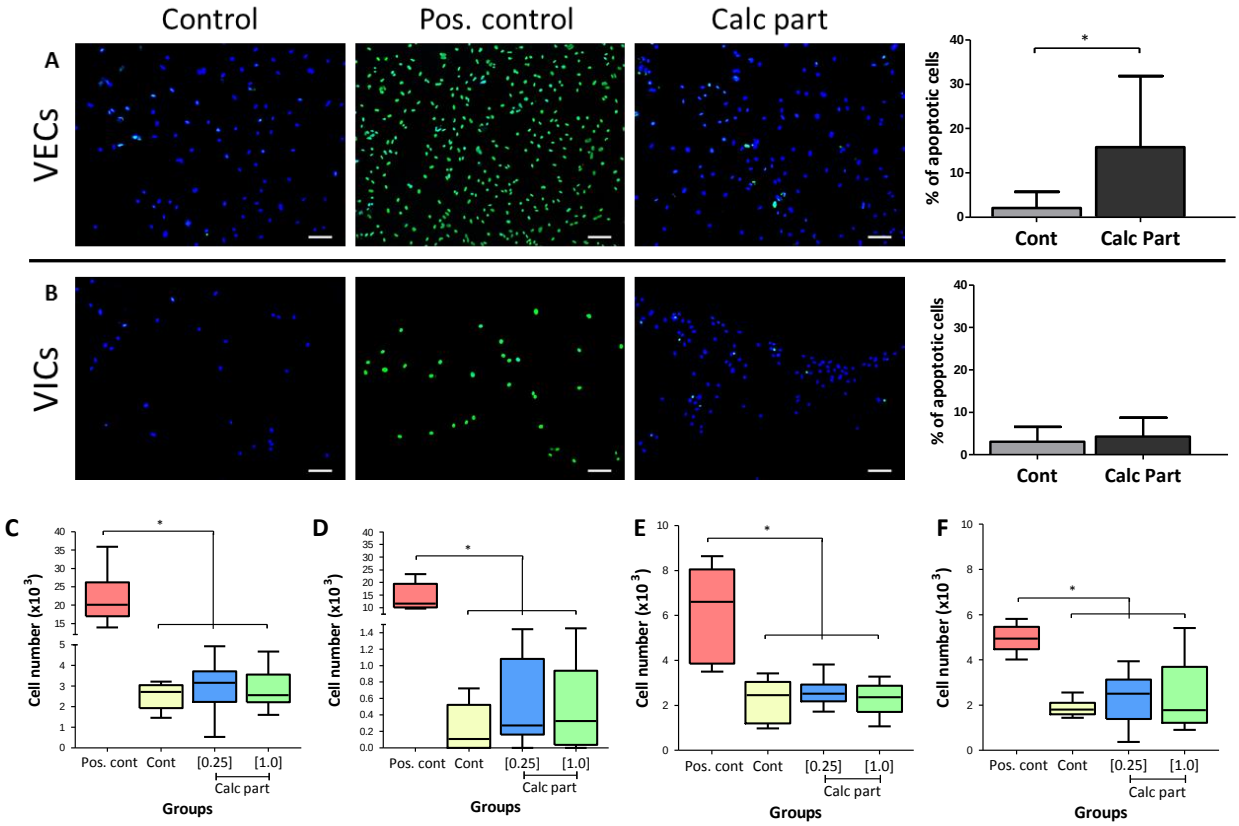

Figure 8. TUNEL staining of VECs (A) and VICs (B) after 7 days of culturing with calcified particles. Green represents apoptotic cells and in blue the nuclei. Scale bars represent 100 µm. Graph showing the proliferation of VECs (C) and VICs (E) after 7 days of culturing and of VECs (D) and VICs (F) after 14 days of culturing with different amounts of particles. For the VECs, in red the positive control (with endothelial media), yellow the control (0.4% FCS in endothelial media without growth factors and particles); for the VICs, in red the positive control (with fibroblast media), yellow the control (0.4% FCS in basal media without treatment of the particles); for both cell types, blue represents OD of 1.0 and green an OD of 0.25 used for the particles. Data are depicted as mean and SD. * $p < 0.05$.

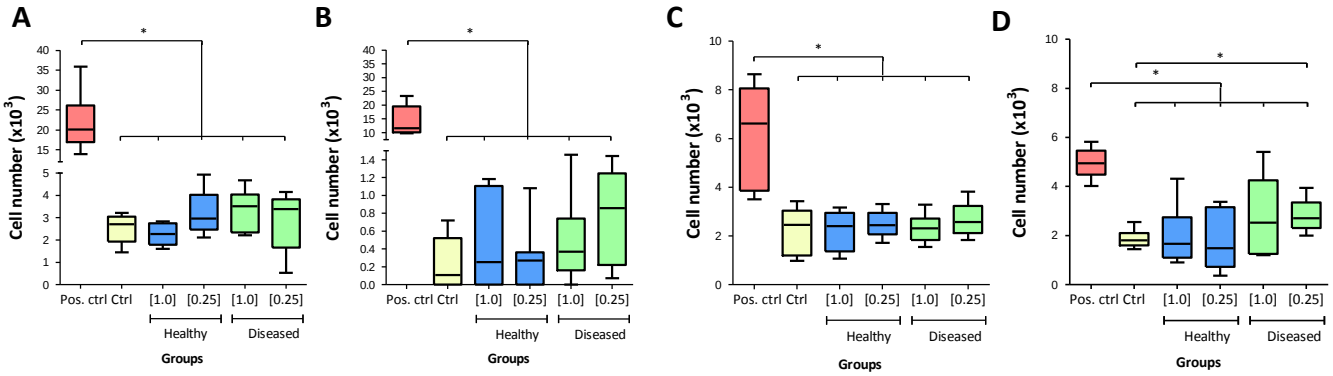

Supplemental Figure 1. Graph showing the proliferation of VECs (A) and VICs (C) after 7 days of culturing and of VECs (B) and VICs (D) after 14 days of culturing with different amounts of particles. For the VECs, in red the positive control (with endothelial media), yellow the control (0.4% FCS in endothelial media without growth factors and particles); for the VICs, in red the positive control (with fibroblast media), yellow the control (0.4% FCS in basal media without treatment of the particles); for both cell types, blue represents a treatment with particles from healthy donors with an OD of 1.0 and 0.25 and green treatment with particles from diseased donors with an OD of 1.0 and 0.25 used for the particles. Data are depicted as mean and SD. * $p < 0.05$.

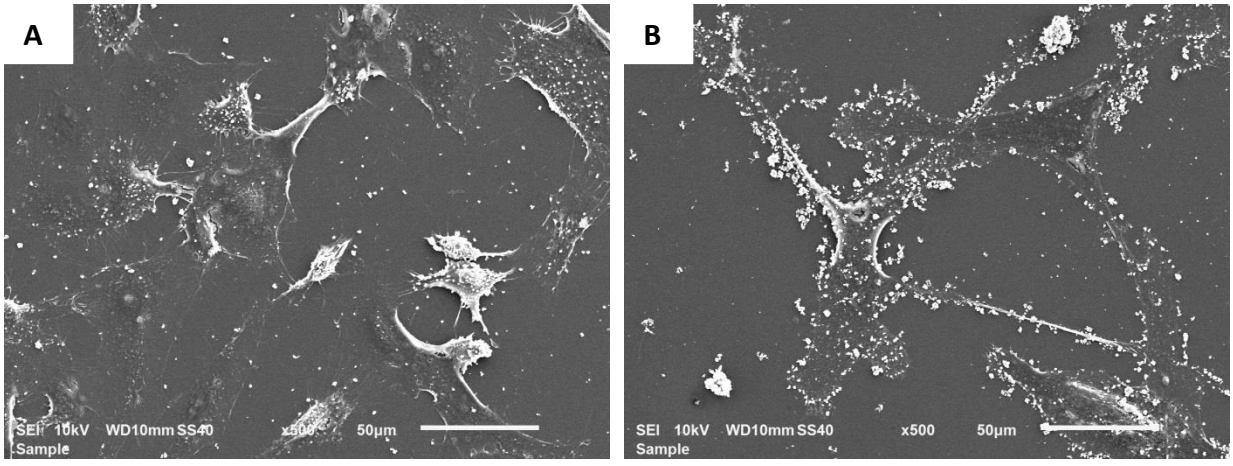

Supplemental Figure 2. Representative SEM micrographs of VECs (A) and VICs (B) after treatment with calcified particles for 7 days. Scale bars indicate 50 µm.